Municipal Solid Waste Gasification with Solid Oxide Fuel Cells and Stirling Engine

Rokni, Masoud

Published in:
Proceedings of the International Conference on Clean Energy 2014

Publication date:
2014

Document Version
Peer reviewed version

ICCE 2014 Conference, Istanbul, Turkey, 8 – 12 June 2014, pp:2431-45.

MUNICIPAL SOLID WASTE GASIFICATION WITH SOLID OXIDE FUEL CELLS AND STIRLING ENGINE

Masoud Rokni
Technical University of Denmark, Dept. of Mechanical Engineering, Thermal Energy Section
Building 403, 2800 Kgs, Lyngby, Denmark
e-mail: MR@mek.dtu.dk

ABSTRACT

Municipal Solid Waste (MSW) can be considered a valid biomass to be used in a power plant. The major advantage is the reduction of pollutants and greenhouse gases emissions not only within large cities but also globally. Another advantage is that by their use it is possible to reduce the waste storage in landfills and devote these spaces to other human activities. It is also important to point out that this kind of renewable energy suffers significantly less availability which characterizes other type of renewable energy sources such as in wind and solar energy.

In a gasification process, waste is subject to chemical treatments through air or/and steam utilization; the result is a synthesis gas, called “Syngas” which is principally composed of hydrogen and carbon monoxide. Traces of hydrogen sulfide could also be present which can easily be separated in a desulfurization reactor. The gasification process is usually based on an atmospheric-pressure circulating fluidized bed gasifier coupled to a tar-cracking vessel. Syngas can be used as fuel in different kind of power plant such as gas turbine cycle, steam cycle, combined cycle, internal and external combustion engine and Solid Oxide Fuel Cell (SOFC).

In the present study, a MSW gasification plant integrated with SOFC is combined with a Stirling engine to recover the energy of the off-gases from the topping SOFC cycle. Detailed plant design is proposed and thermodynamic analysis is performed. Relevant parameters have been studied to optimize the plant efficiency in terms of operating conditions. Compared with modern waste incinerators with heat recovery, the gasification process integrated with SOFC and Stirling engine permits an increase in electricity output up of 50%, which means that the solid waste gasification process can compete with incineration technology. Moreover waste incinerators require the installation of sophisticated exhaust gas cleaning equipment that can be large and expensive and are not necessary in the studied plant.

INTRODUCTION

Due to the ever-increasing demand for more efficient power production and distribution, the main topics of research and development in the field of electricity production are improving efficiency and reducing pollutant emissions. There is currently an increased interest in developing a distributed system of smaller-scale facilities rather than a large-scale facility at a single location, allowing electricity and heat to be produced and distributed close to the end user and thereby minimizing the costs associated with transportation, see (Sanchez et al., 2008) and (Rokni, 2013a).

The word “Biomass” refers to vegetables and animals substances, not from fossil origin; these can be used as fuel in a power plant for the production of electrical energy. Biomasses derive from living or recently living biological organisms and can be considered as a particular kind of renewable energy source, because the carbon dioxide placed in the atmosphere by their use derives from the carbon amount absorbed during their life. In this way, the most important pollutants linked to biomass utilizations are related to transport, manufacture and transformation processes.
Municipal Solid Waste can be considered a valid biomass to use in a power plant. Some advantages can be obtained; the principal is the reduction of pollutants and greenhouse gases emissions. Another advantage is that by their use it is possible to reduce the storage in landfills and devote these spaces to other human activities.

It is also important to point out that this kind of renewable energy suffers significantly less availability which characterizes other type of renewable energy sources such as in wind and solar energy. As proposed in (Morris et al., 1998), with a well management of waste, the following points should be considered:

- prevention of waste generation;
- recycling of waste materials;
- reduction at minimum of landfilling disposal;
- incineration with energy recovery at efficiencies comparable with alternative technologies and sophisticated exhaust gas cleaning equipment;
- gasification processes.

In a gasification process, waste is subject to chemical treatments through air or steam utilization; the result is a synthesis gas, called “syngas” which is principally composed of hydrogen and carbon monoxide. Traces of hydrogen sulfide could also be present which can easily be separated in a desulfurization reactor. The gasification process is usually based on an atmospheric-pressure circulating fluidized bed gasifier coupled to a tar-cracking vessel; the gas produced is then cooled and cleaned. Syngas can be used as fuel in different kind of power plant such as gas turbine cycle, steam cycle, combined cycle, internal and external combustion engine and Solid Oxide Fuel Cell (SOFC).
Solid oxide fuel cell (SOFC) stacks will soon enter the commercialization phase, and small Stirling engines are approaching this phase. It therefore would be interesting to integrate these two technologies into a single system, combining the benefits of each system to establish a new technology. Together with an integrated gasification plant that gasifies MSW in a two-step gasification process, electricity and heat could then be produced in an environmentally friendly way.

SOFCs are one of the most promising types of fuel cells, particularly regarding energy production. They are expected to produce clean electrical energy at high convention rates with low noise and low pollutant emissions (Calise et al., 2006).

To date, studies on syngas from coal and biomass gasification to feed SOFC are carried out, such as (Doherty et al., 2010) and (Ghosh and De, 2006). Using synthetic wood gas for operating of SOFC is also experimentally studied in (Buchinger et al., 2007) which showed that wood gas from air gasification always gave a stable performance while wood gas from steam gasification did not give clear results.

The exhaust temperatures of SOFCs are high due to the high operating temperature of the cells. Additionally, because the fuel utilization in the fuel cell never reaches 100 percent, the unreacted fuel needs to be combusted in a burner. This combustion in turn produces even hotter off-gases that are perfectly suited for use in a heat engine, such as a Stirling engine, for the production of power and heat for domestic purposes.

Numerous studies have investigated SOFC-based power systems and suggested high thermal efficiencies in the literature. However, the majority of these studies use gas turbines as the bottoming cycle, see, e.g., (US Department of energy, 2004), (Riensche et al., 2000) and (Haseli et al. 2008). A steam turbine has also been used as a bottoming cycle (Rokni 2010a and Rokni 2010b), resulting in high plant efficiency. Only a few studies have been carried out with a Stirling engine as a bottoming cycle when a fuel cell cycle is used as the topping cycle, see, e.g., (Sanchez et al., 2008) and (Rokni, 2013a). At present, using the Brayton and Rankine cycles as bottoming cycles seems to be the most practical because of the maturity of these technologies. Given that the development trends suggest that the operating temperature of the SOFC will decrease, using gas turbine as bottoming cycle will become less beneficial over time.

Introducing a heat engine (Stirling) as bottoming cycle for SOFC compared to gas turbine and steam cycles has several advantages. Such hybrid cycle is significantly less complex, heat production will be as much as electrical power (high heat-power ratio), small scale CHP (combined heat and power) plants suitable for hotels, hospitals, shopping centers can be built and the plant cost will be much lower.

Integrated gasification SOFC systems have also been studied, see, for example, (Proell et al., 2004), (Bang-Møller and Rokni, 2010) and (Rokni, 2012). However, there has been an absence of research into integrated MSW gasification SOFC-Stirling CHP plants in the literature, forming the basis of this study.

The present work is an analytical study that conducts a thermodynamic investigation of systems with integrated gasification of MSW, where the syngas is used as fuel for a SOFC plant that also functions as a topping cycle for a Stirling engine using the heat from the off-gasses exhausted from the topping cycle. The system's net capacity is 120 kW, which is suitable for decentralized CPH plants. The gasifier type used for the analysis is based on the Viking two-stage gasifier built at DTU-Risø, which is an autothermal (air-blown) fixed bed gasifier and produces a clean syngas that can be directly fed into a SOFC. More information on the gasifier plant can be found in (Henriksen et al., 2006), (Ahrenfeldt et al., 2006) and (Hofmann et al., 2007). The SOFC is based on a theoretical model with empirical coefficients calibrated from experimental data. The Stirling engine's parameters are chosen by fitting these parameters to a validated feasible engine.

No investigation on municipal solid waste gasification plant integrated with SOFC and Stirling engine has been found in the open literature, and therefore, the current investigation seems to be completely novel and might bring up new ideas on designing new energy system configurations for future applications. It should also be noted that the system presented here was studied thermodynamically and that the objective of this study was not to present or discuss the associated costs. The performances of the various plants are compared in terms of efficiency, fuel consumption and other related parameters. Thus, the main idea is shortly

- Using municipal solid waste to generate electricity through gasification, SOFC and Stirling engine.

PLANT MODEL

The principal components of the plant are the gasification plant, the SOFC plant and the Stirling engine. Through the gasification plant, MSW is converted into syngas which is a mixture of H2, N2, CO, CO2, H2O, CH4 and Ar. The produced syngas is then cleaned to remove the tracks of H2S that could poison the SOFC.

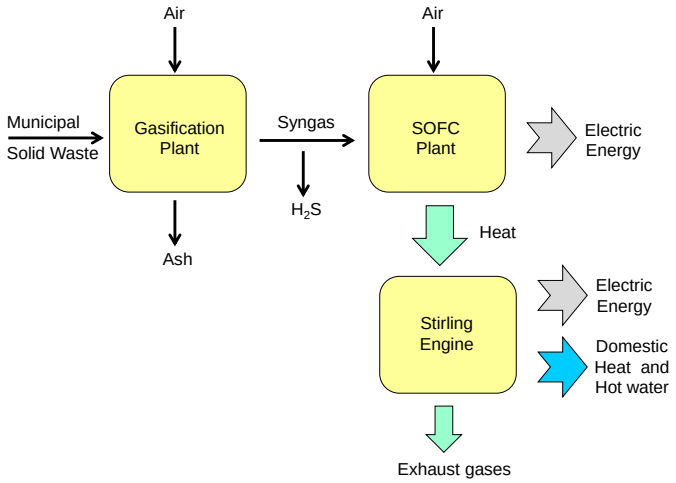

Figure 1. Block scheme of the plant.

The cleaned syngas is then sent to the SOFC plant to produce electricity. The SOFC stacks cannot consume all the fuels and therefore the remaining fuel is sent to the burner to complete the combustion. The combusted gases after the burner are then sent to a Stirling engine (acts as a bottoming cycle) for further electricity production. Both engine cooling circuit and the heat released through the exhausted gases can be used for space heating and domestic hot water (DHW) production, see the block scheme shown in Fig. 1.

Apart from the fuel, the other inputs of the plant are air feeding the gasifier and air feeding the cathode side of the SOFC stacks. To introduce these, auxiliary energy is necessary such as compressors. Another use of auxiliary energy is to blow the syngas out from the gasification plant.

The efficiency of the plant can be expressed as the ratio between the net electric power and the fuel power, where net power refers to the difference between the total produced power and the power used in the auxiliary components such as compressors, blowers, control systems, etc.:

$$\eta = \frac{P_{Net}}{\dot{m}_{fuel} LHV_{fuel}} = \frac{P_{Tot} - P_{Aux}}{\dot{m}_{fuel} LHV_{fuel}} \tag{1}$$

Gasifier and Methanator Modeling

The gasification plant used in this study is based on the model developed in (Rokni, 2012) which is repeated here for the sake of clarification. A simple Gibbs reactor is implemented, meaning that the total Gibbs free energy has its minimum when the chemical equilibrium is achieved. Such characteristic can be used to calculate the gas composition at a specified temperature and pressure without considering the reaction pathways (Smith et al., 2005). The Gibbs free energy of a gas (assumed to be a mixture of *k* perfect gases) is given by

$$\dot{G} = \sum_{i=1}^{k} \dot{n}_i \left[g_i^0 + RT \ln\left(n_i p\right) \right] \tag{2}$$

where g^0, R and T are the specific Gibbs free energy, universal gas constant and gas temperature respectively. Each atomic element in the inlet gas is in balance with the outlet gas composition, which shows that the flow of each atom has to be conserved. For *N* elements, this balance is expressed as, see, e.g. (Rokni, 2012)

$$\sum_{i=1}^{k} \dot{n}_{i,in} \mathbf{A}_{ij} = \sum_{m=1}^{w} \dot{n}_{m,out} \mathbf{A}_{mj} \qquad \text{for } j = 1,N \tag{3}$$

The *N* elements correspond to H_2, O_2, N_2, CO, NO, CO_2, steam, NH_3, H_2S, SO_2, CH_4, C, NO_2, HCN (hydrogen cyanide), COS (carbonyl sulfide), Ar and Ashes (SiO_2) in gasifying process. A_{mi} is the number of atoms of element j (H, C, O, N) in each molecule of entering compound i (H_2, CH_4, CO, CO_2, H_2O, O_2, N_2 and Ar), while A_{ij} is the number of atoms of element *j* in each molecule of leaving compound *m* (H_2, O_2, N_2, CO, NO, CO_2, steam, NH_3, H_2S, SO_2, CH_4, C, NO_2, HCN (hydrogen cyanide), COS, Ar and Ashes). The minimization of the Gibbs free energy can be formulated by introducing a Lagrange multiplier, μ, for each of the *N* obtained constraints. After adding the constraints, the expression to be minimized is then

$$\phi = \dot{G}_{tot,out} + \sum_{j=1}^{N} \mu_j \left(\sum_{i=1}^{k} \dot{n}_{i,out} A_{ij} - \sum_{m=1}^{w} \dot{n}_{m,in} A_{mj} \right) \tag{4}$$

By setting the partial derivation of this equation with respect to $\dot{n}_{i,out}$ to zero then the function φ can be minimized as

$$\begin{aligned} &\frac{\partial \phi}{\partial \dot{n}_{i,out}} = \frac{\partial \dot{G}_{tot,out}}{\partial \dot{n}_{i,out}} + \sum_{j=1}^{N} \mu_j \mathbf{A}_{ij} = 0 \qquad \text{for } i = 1,k \\ &\Rightarrow \quad g_{i,out}^0 + RT \ln\left(n_{i,out} p_{out}\right) + \sum_{j=1}^{N} \mu_j \mathbf{A}_{ij} = 0 \qquad \text{for } i = 1,k \end{aligned} \tag{5}$$

Thus a set of *k* equations were defined for each chemical compound leaving the system.

Finally, it was found that by assuming chemical equilibrium at the gasifier the methane content in the product gas was underestimated. Therefore, a parameter called METHANE was applied to allow some of the methane bypasses the gasifier without undergoing any chemical reactions. By adjusting this parameter the product gas could be calibrated against the experimental data of the Viking gasification plant and found to be 0.01 meaning that 1% of the methane was bypassed in the gasifier, although very small amount, see (Rokni, 2012). Changing the fuel from biomass to municipal waste shall change this parameter slightly but due to lack of experimental data this value was assumed to be the same.

The basic MSW composition and properties used in this study is shown in Table 1, which is based on the study of (Channiwala and Parikh, 2002). This composition should be considered valid unless other values are provided. Note that the compositions are referred to a dry basis, meaning that percentages are expressed in terms of weight fraction without moister content. The MSW composition is then changed as discussed below.

Table 1. Municipal solid waste compositions and properties used in this study.

MSW	Dry-based percentage
C [%]	47.6
H [%]	6
O [%]	32.9
S [%]	0.3
N [%]	1.2
Ash [%]	12
LHV [kW], (dry basis)	19879
c_p [kJ/kg]	1.71
Moisture	0.095

SOFC Modeling

The SOFC model developed in (Rokni, 2012) is used in this investigation, which were calibrated against experimental data for planar SOFC type. For the sake of clarity, it is shortly described here. In such modeling one must distinguish between electrochemical modeling, calculation of cell irreversibility (cell voltage efficiency) and the species compositions at outlet. For electrochemical modeling, the operational voltage (E_{cell}) was found to be

$$E_{cell} = E_{Nernst} - \Delta E_{act} - \Delta E_{ohm} - \Delta E_{conc} \tag{6}$$

where E_{Nernst} , ΔE_{act} , ΔE_{ohm} and ΔE_{conc} are the Nernst ideal reversible voltage, activation polarization, ohmic polarization and concentration polarization. Assuming that only hydrogen is electrochemically converted, then the Nernst equation can be written as

$$E_{Nernst} = \frac{-\Delta g_f{}^0}{n_e F} + \frac{RT}{n_e F} \ln\left(\frac{p_{H_2,tot}\sqrt{p_{O_2}}}{p_{H_2O}} \right) \tag{7}$$

$$p_{H2,tot} = p_{H2} + p_{CO} + 4p_{CH4} \tag{8}$$

where Δg_f^0 is the Gibbs free energy (for H_2 reaction) at standard pressure. Its value is – 38962.24 J/mol at 298.15 K and 1 bar. The water-gas shift reaction is very fast and therefore the assumption of hydrogen as only species to be electrochemically converted is justified, see (Holtappels et al., 1999) and (Matsuzaki and Yasuda, 2000). In the above equations p_{H2} and p_{H2O} are the partial pressures for H_2 and H_2O respectively.

The activation polarization can be evaluated from the Butler–Volmer equation (Keegan et al., 2002), which is isolated from other polarizations to determine the charge transfer coefficients and exchange current density from the experiment by the curve fitting technique.

The ohmic polarization (Zhu and Kee, 2003) depends on the electrical conductivity of the electrodes as well as the ionic conductivity of the electrolyte. This was also calibrated against experimental data for a cell with anode thickness, electrolyte thickness and cathode thickness of 600 μm, 50 μm and 10 μm respectively.

The concentration polarization is dominant at high current densities for anode-supported SOFCs, wherein insufficient amounts of reactants are transported to the electrodes and the voltage is then reduced significantly. Again the concentration polarization was calibrated against experimental data by introducing the anode limiting current, (Costamagna et al., 2004), in which the anode porosity and tortuosity were also included among other parameters.

The fuel composition at anode outlet was calculated using the Gibbs minimization method as described in (Smith et al., 2005). Equilibrium at the anode outlet temperature and pressure was assumed for the following species: H_2, CO, CO_2, H_2O, CH_4 and N_2. Thus the Gibbs minimization method calculates the compositions of these species at outlet by minimizing their Gibbs energy. The equilibrium assumption is fair because the methane content in this study is very low.

To calculate the voltage efficiency of the SOFC cells, the power production from the SOFC (P_{SOFC}) depends on the amount of chemical energy fed to the anode, the reversible efficiency (η_{rev}), the voltage efficiency (η_v) and the fuel utilization factor (U_F). It is defined in mathematical form as

$$P_{SOFC} = \left(\mathrm{LHV}_{H_2}\dot{n}_{H_2,in} + \mathrm{LHV}_{CO}\,\dot{n}_{CO,in} + \mathrm{LHV}_{CH_4}\,\dot{n}_{CH_4,in}\right)\eta_{rev}\,\eta_v\,U_F \tag{9}$$

where U_F was a set value and η_v was defined as

$$\eta_v = \frac{\Delta E_{cell}}{E_{Nernst}} \tag{10}$$

The reversible efficiency is the maximum possible efficiency defined as the relationship between the maximum electrical energy available (change in Gibbs free energy) and the fuels LHV (lower heating value) as follows, (see e.g. Winnick, 1997)

$$\eta_{rev} = \frac{\left(\Delta \bar{g}_f\right)_{fuel}}{\mathrm{LHV}_{fuel}} \tag{11}$$

Additionally, equations for conservation of mass (with molar flows), conservation of energy and conservation of momentum were also included into the model. Table 2 displays the main parameters for the SOFC stacks used in this study.

Table 2. The main SOFC parameters used in this study.

Parameter	Value
Fuel utilization factor	0.675
Number of cells in stack	74
Number of stacks	160
Cathode pressure drop ratio (bar)	0.05
Anode pressure drop ratio (bar)	0.01
Cathode inlet temperature (˚C)	600
Anode inlet temperature (˚C)	650
Outlet temperatures (˚C)	780
Generator efficiency	0.97

Stirling Modeling

The model for Stirling engine used in this study is adopted from the model developed in (Rokni, 2013a), which is a pseudo Stirling cycle, and more closely approximates actual engine performance, developed in (Reader, 1979). A brief explanation of how the model is implemented in the in-house program is herein provided.

The main difference between the pseudo Stirling cycle and the ideal Stirling cycle is the assumption of isentropic compression and expansion in the former rather than isothermal compression and expansion in the latter. It is assumed that isentropic compression and expansion provide more realistic cycle performance because, by incorporating these processes, the losses encountered in the Stirling engine are accounted for. In modeling, the engine is divided into three parts: the heater, engine and a cooler.

The most important parameters of a Stirling engine are the temperature ratio, the compression ratio, the regenerator effectiveness and the heater effectiveness. Engine power can be determined from engine efficiency and the difference between the heat source and heat sink. Heat added to and removed from the engine can be done by two different heat exchangers and their effectiveness. The losses from the Stirling engine are the result of various loss mechanisms, including mechanical and thermal processes. Therefore, a “loss factor” is incorporated that accounts for all mechanisms of losses in the engine, including both mechanical and thermal.

The highest temperature of the working fluid (helium) is lower than the heater wall temperature, and the lowest temperature of the working fluid is a weighted temperature and is the average between the inlet and outlet temperatures. Therefore, ΔT_{heater} and ΔT_{cooler} are introduced which refer to the temperature difference over the heater and cooler, respectively. The main parameters for the Stirling engine used in this study are shown in Table 3.

Table 3. The main Stirling engine parameters used in this study.

Parameter	Value
Heater and cooler Δp (bar)	0.01
Heater wall temperature (˚C)	600
Heater ΔT (˚C)	125
Heater effectiveness	0.95
Cooler ΔT (˚C)	60
Compressor ratio (–)	1.44
Regenerator effectiveness	0.98
Mechanical loss factor	0.8

Modeling of Other Components

Modeling of other components such as heat exchangers, pumps, desulfurization reactor, etc. are adopted from the study of (Rokni, 2013a), in which the reliability of the components modeling was justified by building a benchmark system consisting SOFC, methanator, heat exchanger, etc. and fed with different fuels such as natural gas, ethanol, methanol and di-methyl ether (DME). The obtained results agreed well with the corresponding data obtained by other researchers in the open literature for all cases studied.

PLANT CONFIGURATION

The system investigated here is presented in Fig. 2, which is a small-scale CHP consisting of an integrated MSW gasification plant with an SOFC system functioning as a topping cycle, while a Stirling engine with domestic hot water

heaters comprises the bottoming cycle. Such small scale consisting of a MSW gasification integrated with SOFC-Stirling which has a high heat-power ratio is has not been investigated previously. MSW are fed into a gasifier for the production of syngas via a two-step process. The first step is a pyrolysis of the feedstock, and the second step utilizes a fixed bed gasifier, where the pyrolysed feedstock is gasified by steam and air as gasification agents. A gas cleaner is introduced to remove the small contaminants present in the syngas, mainly sulfur. The operating temperature of the gas cleaner is assumed to be about 250°C.

For the topping SOFC cycle, the ambient air at 15°C is compressed to the working pressure of the SOFC (normal pressure) and then heated in the cathode air preheater (CP) to 600°C before entering the cathode side of the SOFC stacks. The cathode preheater uses some of the SOFC off-air to heat the incoming air. The off-air is split into two streams: one entering the CP and the other entering the catalytic burner. For the anode side, the cleaned syngas is first pumped to compensate for the pressure drop along its way. The syngas is then preheated to about 650°C before entering the anode side of the SOFC using the off-fuel out of the fuel cell. The operating temperature of the fuel cell is assumed to be 780°C which is enough to preheat the incoming syngas. The burner is implemented because all of the fuel will not be reacted in the fuel cell stacks due to fuel utilization. The entering temperatures mentioned above are the minimum entering temperatures and are essential requirements for the proper functioning of SOFC stacks, not only to initiate the chemical reactions but also to avoid cell thermal fractures.

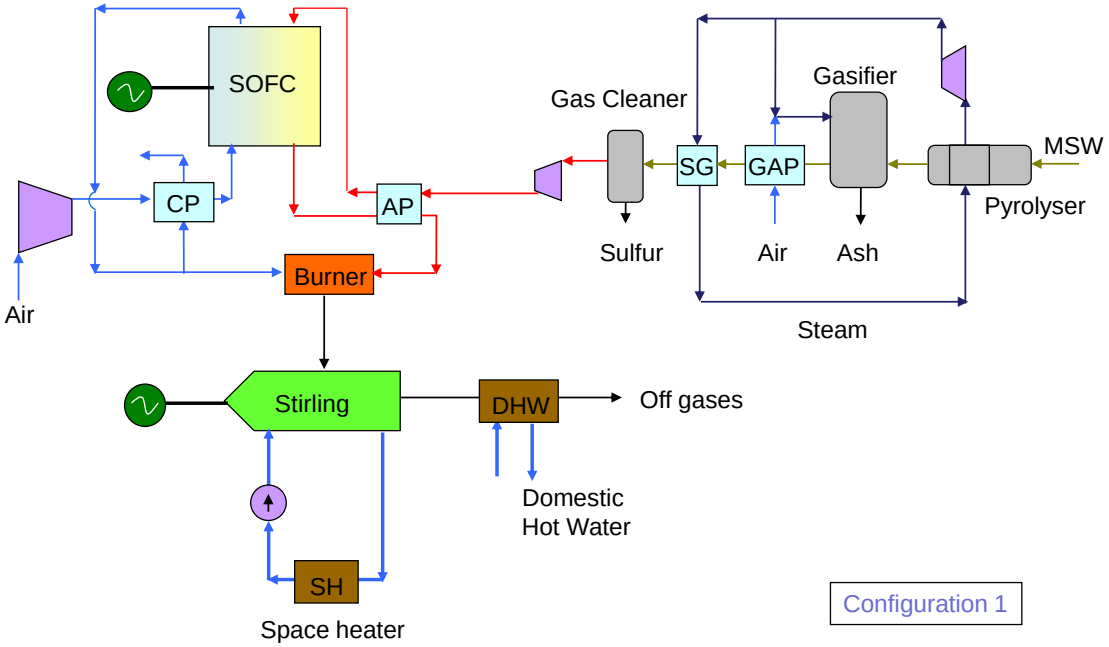

Figure 2. Basic plant configuration.

Table 4. System operating input parameters.

MSW temperature (°C)	15
Pyrlosis temperature (°C)	150
Gasifier temperature (°C)	800
Gasifier pressure (bar)	1
Gasifier pressure drop (bar)	0.005
Gasifier carbon conversion factor	1
Gasifier non-equilibrium methane	0.01
Steam blower isentropic efficiency	0.8
Steam blower mechanical efficiency	0.98
Air temperature into gasifier (°C)	15
Syngas blower isentropic efficiency	0.7
Syngas blower mechanical efficiency	0.95
Syngas cleaner pressure drop	0.0049
Cathode compressor air intake temperature (°C)	15
Compressor isentropic efficiency	0.7
Compressor mechanical efficiency	0.95
Gas heat exchangers pressure drop	0.01
Pinch temperature for cathode preheater (°C)	20
Burner inlet outlet pressure ratio	0.97
Water pump efficiency	0.95
Inlet water temperature for hot water (°C)	20
Outlet water temperature for hot water (°C)	60
Off gas temperature after water heater (°C)	95

For the bottoming cycle, a Stirling engine is implemented. The Stirling engine utilizes the combustion products, leaving the burner as a heat source. The water used as the heat sink enters at 20°C and exits at 60°C, making it appropriate for, both domestic hot water and space heating. In particular, its temperature is sufficient to address problems related to bacteria, e.g., Legionella. The heat remaining after the Stirling engine is used for domestic hot water production. Water is constrained in the same manner as the heat sink, and the combustion products leave the system into the environment at approximately 95°C, which is hot enough to avoid corrosion problems. Other system operating parameters are mentioned in Table 4.

In another configuration it is proposed to include a methanator after the fuel pump and thereby increase the methane contain of the syngas, see Fig. 3. Thus the syngas is reformed exothermically in a methanator, wherein the CH_4 content in the gas is increased from a molar fraction of approximately 0.01 to nearly 0.05, which is the result of the reaction between H_2 and CO. Introducing methanator will decrease electrical production from the SOFC stacks slightly, but on the other hand, because the reformation is highly exothermic, less heat needs to be extracted from the SOFC off-fuel to heat the incoming fuel to the fuel cell. This will eventually provide the Stirling engine with a larger amount of heat to be used because the fuel will be at a higher temperature when entering the burner, and the combustion processes will therefore occur at a higher temperature.

Secondly, the use of a larger molar fraction of CH_4 in the SOFC causes endothermic internal reforming, reducing the amount of air used for cooling purposes and maintaining the SOFC operating temperature at 780°C. Thus, the workload of the cathode compressor will decrease.

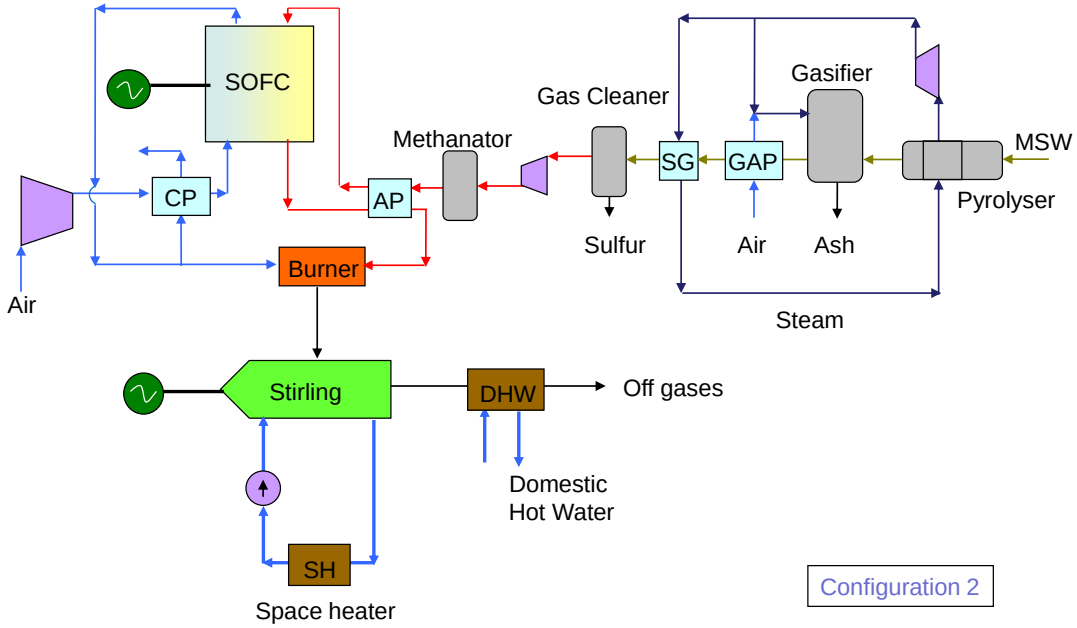

Figure 3. Improved plant configuration by introducing a methanator into the basic configuration.

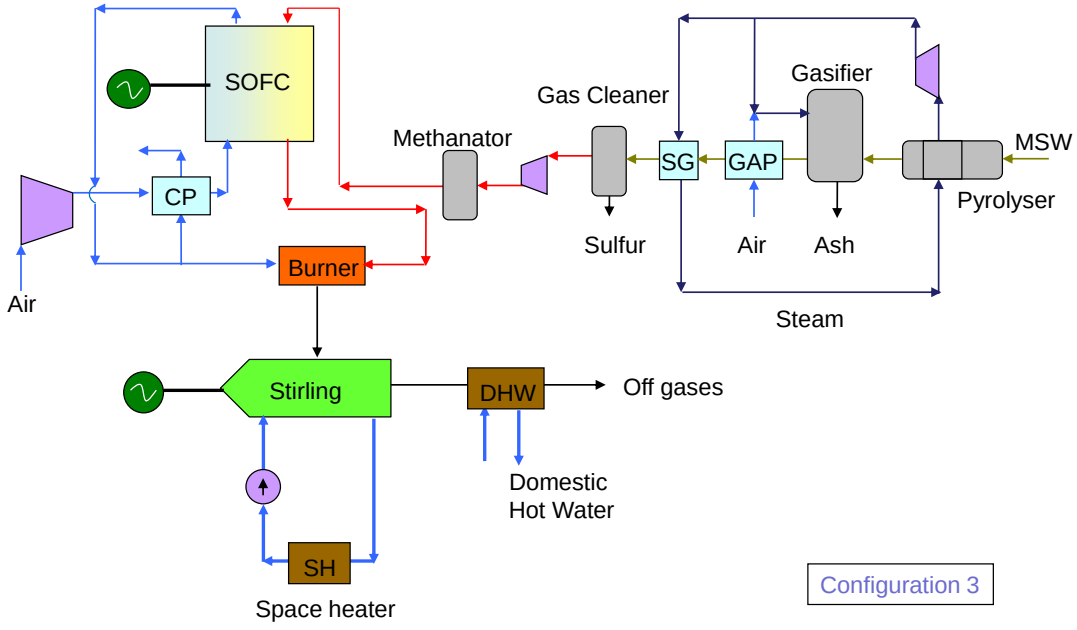

Figure 4. Final plant configuration when methanator is included and anode preheater is removed.

As mentioned above, including a methanator after the fuel pump causes exothermic reformation of the syngas and thereby increasing its temperature. The calculations show that the syngas temperature after the methanator will be higher than the required 650°C, resulting in elimination of anode preheater. Figure 4 shows the final configuration when the anode preheater is replaced by a methanator.

RESULTS AND CONCLUSIONS

The performances of the plants proposed above are shown in Table 5. In the table configuration 1 denotes the basic configuration without methanator. Configuration 2 is the basic plant when a methanator is introduced and anode preheater is kept. Configuration 3 is the final one when a methanator is introduced and the anode preheater is removed. As shown in the table, the electrical efficiency of the final plant is more than 1 percent point higher than the basic one. Electricity production by the SOFC is decreased while power from Stirling engine is increased and auxiliary power consumption is decreased, as the direct result of methanator inclusion. On the other hand both space heating and hot water production will also decrease when a methanator is included. Removing or keeping the anode preheater does not have a significant effect on plant efficiency, power and heat production. As shown in the table, the methanator has two major benefits for the plant, first heat need to preheat the fuel will be decreased resulting in higher heat available for the Stirling engine (through higher burner temperature). Second, compressor load decreases due to lower cooling effect for fuel cells to maintain its operating temperature at the desired level.

Table 5. Plant performance for different configurations.

Configuration	Configuration 1	Configuration 2	Configuration 3
Electrical efficiency, (%)	45.03	45.98	46.07
Plant electrical power, (kW	120	120	120
SOFC power	101.2	99.11	98.91
Stirling power, (kW)	24.94	26.23	26.17
Auxiliary power, (kW	6.097	5.340	5.088
Space heating, (kJ/s)	67.08	60.37	60.09
DHW, (kJ/s)	66.96	60.26	60.26
Total heat, (kW)	134.04	120.63	120.35
CHP efficiency, (%)	95.33	92.20	92.27
MSW mass flow, (kg/h)	54.02	52.91	52.81
Methane content, (molar %)	0.0134	0.0456	0.0460
Burner temperature, (°C)	1288.9	1405.8	1407.7

Configuration 1: basic plant without methanator
Configuration 2: basic plant with methanator and anode preheater
Configuration 3: basic plant with methanator but without anode preheater

Effect of MSW composition

The MSW composition can be changed depending on the garbage type and national recycling policy. In fact MSW composition could change day by day and it could be interesting to investigate different MSW composition feeding to the gasifier and study their effect on plant performance. Therefore, a various MSW compositions presented in the literature is studied here and the results are shown in Table 6.

Table 6. Plant performance with different waste compositions; basic (Channiwala and Parikh, 2002), waste 1 (Buah et al. 2007), waste 2 to 5 (Cozzani et al., 1995), waste mean

Compound	Basic	Waste 1	Waste 2	Waste 3	Waste 4	Waste 5	Waste Mean
C	0.476	0.40	0.459	0.483	0.408	0.422	0.491
H	0.06	0.069	0.068	0.076	0.067	0.061	0.063
O	0.329	0.354	0.337	0.316	0.389	0.399	0.323
S	0.003	0.001	0.0	0.001	0.006	0.001	0.002
N	0.012	0.006	0.011	0.006	0.009	0.008	0.007
Ash	0.12	0.17	0.123	0.116	0.114	0.104	0.114
Cl	–	–	0.002	0.002	0.007	0.005	–
LHV, (kW), (dry basis)	19879	18900	18992	21314	15956	15639	19553
c_p , (kJ/kg)	1.71	1.93	1.85	1.96	1.84	1.74	1.76
Moisture	0.095	0.04	0.04	0.045	0.155	0.04	0.073

In the table “waste mean” represents the mean composition of 19 different waste compositions provided by 12 different references as, (Buah et al., 2007), (Cozzani et al., 1995), (Guan et al., 2009), (Bebar et al., 2005), (Dalai K. et al., 2009), (Galvagno et al., 2009), (Gordillo and Annamalai, 2010), (Baggio et al., 2009), (Hernandez-Atonal et al., 2007), (Piao et al., 1998), (Piao et al., 2000), (Channiwala and Parikh, 2002). Thus, a huge number of data are analyzed and the results are presented as mean composition values for MSW. The experimental values for LHV of the MSWs are given in some references but such value is missing in the other references. The LHV (dry basis) value of the missing MSW is calculated from,

$$\mathrm{LHV} = \mathrm{HHV} - (\mathrm{H} \times 2500) - (\mathrm{Moisture} \times 2500) \quad (12)$$

where HHV is the higher heating value. The moisture of MSW is provided in the corresponding reference and H is the weight percentage of hydrogen. HHV of the MSW is calculated from "Dulong" expression (Channiwala and Parikh, 2002) as

$$\mathrm{HHV} = 0.3383\times \mathrm{C} + 1.443\times(\mathrm{H} - \mathrm{O}/8) + 0.0942\times \mathrm{S} \qquad \mathrm{MJ/kg}. \tag{13}$$

In this expression C, H, O and S are the weight percentage of carbon, hydrogen, oxygen and sulfur, respectively. The heat capacity is calculated from the weighted average of the values of all the elementary components in the fuel;

$$c_{p,fuel} = \frac{\sum_i x_i c_{p,i}}{\sum_i x_i} \tag{14}$$

where x_i are the mass fractions of every component and $c_{p,i}$ is the specific heat capacity of each elementary component. The values for specific heat capacity of each component are adopted from (Incropera et al., 2006) at a temperature of 300K.

The calculations results are shown in Table 7. As shown in the table the electrical efficiency of the plant changes from about 43.6% to about 48.1% depending on the MSW composition. The lowest plant efficiency is obtained with "waste 5" while the highest plant efficiency attained with the "waste 1". The mean waste composition gives a plant efficiency of about 45.1%. Generally, plant efficiency is increased when SOFC cell efficiency is higher and its current density is lower. This can also be visualized in Fig. 5.

Table 7. Plant performance with different MSW compositions.

Waste Type	Electrical Efficiency (%)	SOFC E_{cell} (V)	SOFC Current density (A/cm^2)
Basic	46.07	0.786	0.7382
Waste 1	48.40	0.804	0.7247
Waste 2	45.38	0.776	0.7469
Waste 3	45.89	0.785	0.7399
Waste 4	43.69	0.741	0.7751
Waste 5	43.59	0.751	0.7663
Waste mean	45.13	0.772	0.7494

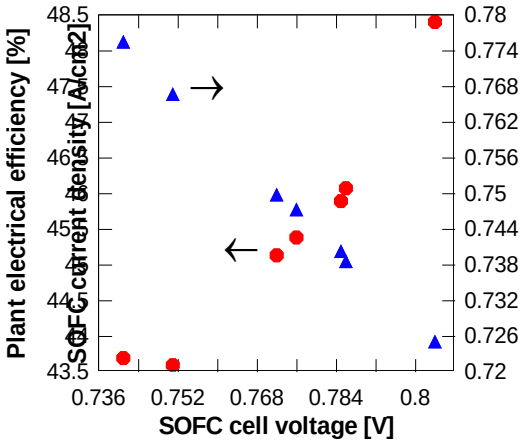

Figure 5. Plant efficiency versus cell voltage and current density with different municipal solid wastes.

Effect of Number of Stacks and Utilization Factor

Both number of stacks and utilization factor have considerable effect on plant performance in term of electrical efficiency. As discussed in (Rokni, 2013b), increasing number of stacks is in favor for plant efficiency. The plant cost is also directly depended on number of stacks and therefore for choosing number of stacks one should also study the economy of the plant, either in terms of thermoeconomy or technoeconomy. Figure 6 demonstrates this effect. For SOFC utilization factor of 0.675 the electrical efficiency increases from about 45.1% to about 47.5% for 100 and 4000 number of stacks respectively. Similarly, cell voltage increases from 0.766 to 0.816. Of course, it is not economical to design the plant with 4000 stacks when power output is only 120 kW, see Fig. 6a. As can be seen in the figure, plant efficiency as well as cell voltage does increase significantly when number of stacks is more than 1000.

Increasing utilization factor to 0.8 show also similar trend. Plant efficiency sharply increases from about 47.5% to about 48% when number of stacks is increased to about 3000. Further increasing the number of stacks has small influence on plant efficiency. It is possible to reach an electrical efficiency of about 48.2% when number of stacks is

about 80000. Again, this would not be economical. Choosing number of stacks to about 150 or 160 will be more viable and this why in the above calculations 160 stacks was chosen.

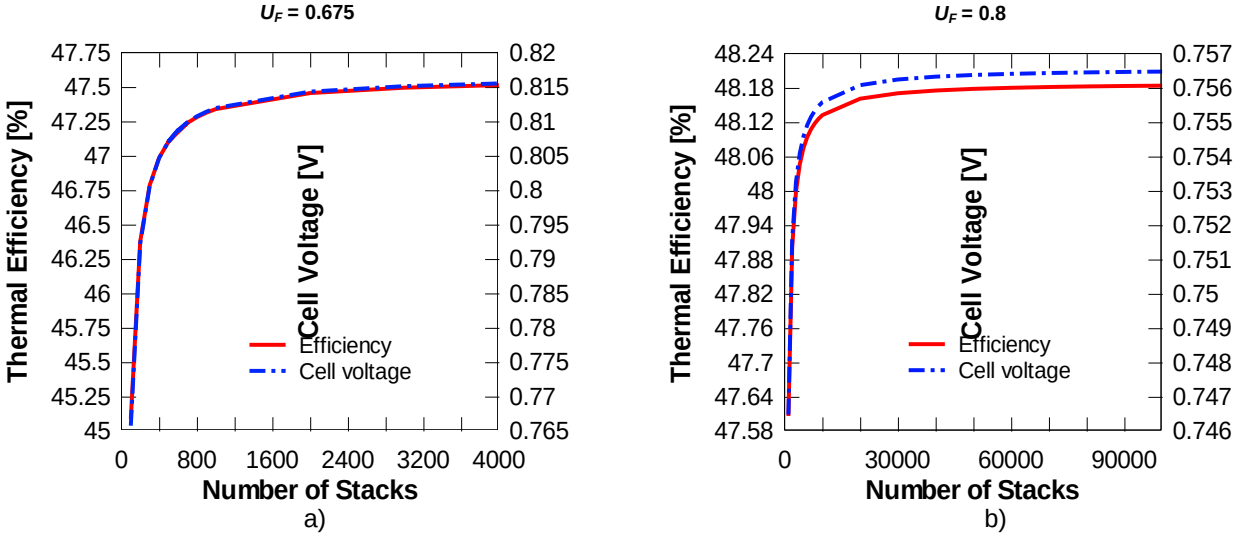

Figure 6. Effect of number of stacks on plant efficiency and cell voltage, for utilization factor, U_F, of 0.675 (a) and 0.8 (b).

CONCLUSIONS

An integrated municipal solid waste gasification combined with SOFC and Stirling engine for decentralized CHP plant of 120 kW electricity power is presented and thermodynamically studied. Plant electrical efficiency up to 48% and CPH efficiency up to 95% is possible to attain, depending on the plant design and MSW composition.

It is shown that applying a methanator after the syngas offers two main advantages, air compressor workload decreases due to less cooling requirement for SOFC stacks. Secondly, less heat will be needed to preheat the incoming fuel to the SOFC offering higher heat available for bottoming cycle and increasing its electricity power production. Despite less fuel cell voltage, plant electrical efficiency increases with such methanator.

Different MSW compositions provide different plant efficiency which ranges from 43 to 48% when 7 different MSW compositions are used in the simulations.19 different MSW compositions are then screened to find out a mean composition and study its effect on plant performance which shown to be about 45% electrical efficiency.

NOMENCLATURE

c_p	specific heat, J/kg°C
E	Voltage, V
F	Faradays constant, C/mol
g^0	Standard Gibbs free energy, J/mol
g_f	Gibbs free energy, J/mol
$\dot{m}$	Mass flow, kg/s
$\dot{n}$	Molar reaction rate, mol/s
n_e	number of electron
P	Power, W
p	Pressure, bar
T	Operating temperature, K
R	Universal gas constant, J/mol K
U_F	Fuel utilization factor
x	mass fraction

Greek Letters

Δ	difference
η	efficiency

Subscripts

act	activation
conc	concentration
ohm	ohmic
rev	reversible
v	voltage

Abbreviations

AP	Anode pre-heater

CHP	Combined heat and power
CP	Cathode air pre-heater
GAP	Gasifier air pre-heater
HHV	Higher heating value
LHV	Lower heating value
MSW	Municipal solid waste
SG	Steam generator
SOFC	Solid oxide fuel cell
SH	Space heater
DHW	Domestic hot water

REFERENCES

[1] Ahrenfeldt J., Henriksen U., Jensen T.K., Gøbel B., Wiese L., Kather A. and Egsgaard H. 2006. Validation of a continuous combined heat and power (CHP) operation of a two-stage boimass gasifier. *Energy and Fuels* 20(6):2672–80.
[2] Baggio P., Baratieri M., Fiori L., Grigiante M., Avi D. and Tosi P. 2009. Experimental and modeling analysis of a batch gasification/pyrolysis reactor. *Energy Conversion and Management* 50(6);1426-35.
[3] Bang-Møller C. and Rokni M. 2010. Thermodynamic performance study on biomass gasification, solid oxide fuel cell and micro gas turbine hybrid systems. *Energy Conversion and Management* 51(12):2330–39.
[4] Bebar L., Stehlık P., Havlen L. and Oral J. 2005. Analysis of using gasification and incineration for thermal processing of wastes. *Applied Thermal Engineering* 25(7);1045-55.
[5] Buah W.K., Cunliffe A.M. and Williams PT. 2007. Characterization of products from the pyrolysis of municipal solid waste. *Process Safety and Environmental Protection* 85(B5);450–57.
[6] Buchinger G., Hinterreiter P., Raab T., Griesser S., Lawlor V,Klein K., Kuehn S., Sitte W. and Meissner D. 2007. Stability of micro tubular SOFCs operated with synthetic wood gases and wood gas components. *IEEE* 1-4244-0632-3/07:444–449.
[7] Calise F., Dentice d'Accadia M., Palombo A. and Vanoli L. 2006. Simulation and exergy analysis of a hybrid solid oxide fuel cell (SOFC)–Gas turbine system. *Energy* 31:3278–99.
[8] Channiwala S.A. and Parikh P.P. 2002. A unified correlation for estimating HHV of solid, liquid and gaseous fuels. *Fuel* 81(8);1051-63.
[9] Costamagna P., Selimovic A., Del Borghi M. and Agnew G. 2004. Electrochemical model of the integrated planar solid oxide fuel cell (IP-SOFC). *Chemical Engineering* 102(1):61–69
[10] Cozzani V., Petarca L. and Tognotti L. 1995. Devolatilization and pyrolysis of refuse derived fuels: characterization and kinetic modelling by a thermogravimetric and calorimetric approach. *Fuel* 74(6);903-12.
[11] Dalai K., Batta N., Eswaramoorthi I. and Schoenau G.J. 2009. Gasification of refuse derived fuel in a fixed bed reactor for syngas production. *Waste Management* 29(1);252-8.
[12] Doherty W., Reynolds A. and Kennedy D. 2010. Computer simulation of a biomass gasification-solid oxide fuel cell power system using Aspen Plus. *Energy* 35(12):4545–55.
[13] EG&G and G Technical Services Inc. 2004*. Fuel Cell Handbook*, 7th edition, U.S. Departement of Energy, Office of Fossil Energy, National Energy Technology Laboratory.
[14] Galvagno S., Casciaro G., Casu S., Martino M., Mingazzini C., Russo A. and Portofino S. 2009. Steam gasification of tyre waste, poplar, and refuse-derived fuel: A comparative analysis. *Waste Management* 29(2);678-89.
[15] Ghosh S. and De S. 2006. Energy Analysis of a cogeneration plant using coal gasification and solid oxide fuel cell. *Energy* 31(2–3),345–363.
[16] Gordillo G. and Annamalai K. 2010. Adiabatic fixed bed gasification of dairy biomass with air and steam. *Fuel* (89(2);384-91.
[17] Guan Y., Luo S., Liu S., Xiao B. and Cai L. 2009. Steam catalytic gasification of municipal solid waste for producing tar-free fuel gas. *Hydrogen Energy* 34(23):9341-46.
[18] Haseli Y., Dincer I. and Natere G.F. 2008. Thermodynamic modeling of a gas turbine cycle combined with a solid oxide fuel cell. *Hydrogen Energy* 33(20):5811-22.
[19] Henriksen U., Ahrenfeldt J., Jensen T.K., Gøbel B., Bentzen J.D., Hindsgaul C. and Sørensen L.H. 2006. The design, construction and operation of a 75 kW two-stage gasifier. *Energy* 31(10–11):1542–53.
[20] Hernandez-Atonal F.D., Ryu C., Sharifi V.N. and Swithenbank J. 2007. Combustion of refuse-derived fuel in a fluidised bed. *Chemical Engineering Science* 62(1-2);627-35.
[21] Hofmann P.H., Schweiger A., Fryda L., Panopoulos K., Hohenwarter U., Bentzen J., Ouweltjes J.P., Ahrenfeldt J., Henriksen U. and Kakaras E. 2007. High temperature electrolyte supported Ni-GDC/YSZ/LSM SOFC operation on two stage Viking gasifier product gas. *Power Sources* 173(1):357–366.
[22] Holtappels P., DeHaart L.G.J., Stimming, U., Vinke I.C. and Mogensen M. 1999. Reaction of CO/CO2 gas mixtures on Ni-YSZ cermet electrode. *Appl. Electrochem.* 29:561-68.
[23] Incropera F.P., DeWitt D.P., Bergman TL and Lavine A.S. 2006. *Introduction to Heat Transfer*. 5th ed, Wiley, ISBN 978-0471457275.
[24] Keegan K.M., Khaleel M., Chick L.A., Recknagle K., Simner S.P. and Diebler J. 2002. Analysis of a planar solid oxide fuel cell based automotive auxiliary power unit, *SAE Technical Paper Series* No. 2002-01-0413.
[25] Matsuzaki Y. and Yasuda I. 2000. Electrochemical oxidation of H2 and CO in a H2-H2O-CO-CO2 system at the interface of a Ni-YSZ cermet electrode and YSZ electrolyte. *Electrochemistry Society* 147(5):1630–35.

[26] Morris M. and Waldheim L. 1998. Energy recovery from solid waste fuels using advanced gasification technology. *Waste Management* 18(6-8):557-564.
[27] Piao G., Aono S., Mori S., Deguchi S., Fujima Y., Kondoh M. and Yamaguchi M. 1998. Combustion of refuse derived fuel in a fluidized bed. *Waste Management* 18(6-8);509-12.
[28] Piao G., Aono S., Kondoh M., Yamazaki R. and Mori S. 2000. Combustion test of refuse derived fuel in a fluidized bed. *Waste Management* 20(5-6); 443-7.
[29] Proell T., Aichering C., Rauch R. and Hofbauer H. 2004. Coupling of biomass steam gasification and SOFC-gas turbine hybrid system for highly efficient electricity generation. *ASME turbo Expo Proceeding*;GT2004-53900:103-112.
[30] Reader G.T. 1979. The pseudo Stirling cycle – a suitable performance criterion. *Proceeding of the 13th intersociety energy conversion engineering conference*. Vol. 3:1763–770, San Diego, California, August 20–25.
[31] Riensche E., Achenbach E., Froning D., Haines M.R., Heidug W.K., Lokurlu A. and Adrian S. 2000. Clean combined-cycle SOFC power plant–cell modeling and process analysis. *Power Sources* 86(1–2):404–410.
[32] Rokni M. 2010a. Thermodynamic analysis of an integrated solid oxide fuel cell cycle with a Rankine cycle. *Energy Conversion and Management* 51(12):2724–32.
[33] Rokni M. 2010b. Plant characteristics of an integrated solid oxide fuel cell and a steam cycle. *Energy* 35:4691–99.
[34] Rokni M. 2012. Thermodynamic investigation of an integrated gasification plant with solid oxide fuel cell and steam cycles. *Green* 2:71–86.
[35] Rokni M. 2013a. Thermodynamic analysis of SOFC (solid oxide fuel cell) – Stirling hybrid plants using alternative fuels. *Energy* 61:87–97.
[36] Rokni M. 2013b. Thermodynamic and thermoeconomic investigation of an integrated gasification SOFC and Striling engine, *SDEWES2013 Conference*, Dubrovnik, Croatia, pp:0166-1 to 0166-23.
[37] Smith J.M., Van Ness H.C. and Abbott M.M. 2005. *Introduction to Chemical Engineering Thermodynamics*, 7th edition, Boston:McGraw-Hill.
[38] Sanchez D., Chacartegui R., Torres M. and Sanchez T. 2008. Stirling based fuel cell hybrid systems: an alternative for molten carbonate fuel cells. *Power Sources* 192:84–93.
[39] Zhu H. and Kee R.J. 2003. A general mathematical model for analyzing the performance of fuel-cell membrane-electrode assemblies. *Power Sources* 117:61–74.
[40] Winnick J. 1997. *Chemical engineering thermodynamics*. John Wiley &Sons, New Yourk.